BIOCHEMISTRY
including biophysical chemistry & molecular biology

Article

pubs.acs.org/biochemistry

# Replication, Repair, and Translesion Polymerase Bypass of $N^6$-Oxopropenyl-2′-deoxyadenosine

Leena Maddukuri,[†] Sarah C. Shuck,[†] Robert L. Eoff,[∥] Linlin Zhao,[⊥] Carmelo J. Rizzo,[‡]
F. Peter Guengerich,[†] and Lawrence J. Marnett*[,†,‡,§]

A. B. Hancock Jr. Memorial Laboratory for Cancer Research, [†]Department of Biochemistry, [‡]Department of Chemistry, and [§]Department of Pharmacology, Center in Molecular Toxicology, Vanderbilt Institute of Chemical Biology, and Vanderbilt-Ingram Cancer Center, Vanderbilt University School of Medicine, Nashville, Tennessee 37232-0146, United States

[∥]Department of Biochemistry and Molecular Biology, University of Arkansas for Medical Sciences, Little Rock, Arkansas 72205-7199, United States

[⊥]Department of Chemistry, Central Michigan University, Mt. Pleasant, Michigan 48859, United States

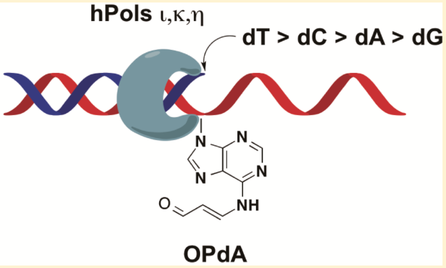

**ABSTRACT:** The oxidative stress products malondialdehyde and base propenal react with DNA bases forming the adduction products 3-(2′-deoxy-*β*-D-*erythro*-pentofuranosyl)pyrimido[1,2-*a*]purin-10(3*H*)-one ($M_1dG$) and $N^6$-(oxypropenyl)-2′-deoxyadenosine (OPdA). $M_1dG$ is mutagenic *in vivo* and miscodes *in vitro*, but little work has been done on OPdA. To improve our understanding of the effect of OPdA on polymerase activity and mutagenicity, we evaluated the ability of the translesion DNA polymerases hPols $\eta$, $\kappa$, and $\iota$ to bypass OPdA *in vitro*. hPols $\eta$ and $\kappa$ inserted dNTPs opposite the lesion and extended the OPdA-modified primer to the terminus. hPol $\iota$ inserted dNTPs opposite OPdA but failed to fully extend the primer. Steady-state kinetic analysis indicated that these polymerases preferentially insert dTTP opposite OPdA, although less efficiently than opposite dA. Minimal incorrect base insertion was observed for all polymerases, and dCTP was the primary mis-insertion event. Examining replicative and repair polymerases revealed little effect of OPdA on the *Sulfolobus solfataricus* polymerase Dpo1 or the Klenow fragment of *Escherichia coli* DNA polymerase I. Bacteriophage T7 DNA polymerase displayed a reduced level of OPdA bypass compared to unmodified DNA, and OPdA nearly completely blocked the activity of base excision repair polymerase hPol $\beta$. This work demonstrates that bypass of OPdA is generally error-free, modestly decreases the catalytic activity of most polymerases, and blocks hPol $\beta$ polymerase activity. Although mis-insertion opposite OPdA is relatively weak, the efficiency of bypass may introduce A → G transitions observed *in vivo*.

Cellular production of reactive oxygen species poses a significant threat to genomic stability by inducing DNA damage, a contributing factor in carcinogenesis.[1] Endogenous DNA damage can be induced directly by the oxidation of DNA bases or by secondary mechanisms in which cellular targets are oxidized to products that subsequently damage DNA.[1] Lipids represent a major target for oxidant attack, leading to fatty acid breakdown and the formation of $\alpha,\beta$-unsaturated aldehydes, including malondialdehyde (MDA) and acrolein.[2] Reactive oxygen species also react with the DNA backbone, leading to the formation of base propenal, which further modifies DNA bases.[3] The reaction of MDA or base propenal with DNA leads to the formation of a variety of adducts, including 3-(2′-deoxy-*β*-D-*erythro*-pentofuranosyl)pyrimido[1,2-*a*]purin-10(3*H*)-one ($M_1dG$), $N^6$-(oxopropenyl)-2′-deoxyadenosine (OPdA), and $N^4$-(oxopropenyl)-2′-deoxycytidine (OPdC) (Figure 1).[2,4,5] $M_1dG$ is the major product of MDA and base propenal DNA modification, whereas OPdA and OPdC are minor products.[6] $M_1dG$ is a ring-closed, exocyclic DNA adduct, whereas OPdA and OPdC represent ring-opened DNA adducts (Figure 1).

DNA adducts can induce mutations and impair the activity of proteins important in genomic maintenance. When $M_1dG$ is present in duplex DNA opposite dC, the exocyclic ring opens, forming $N^2$-(oxopropenyl)-2′-deoxyguanosine ($N^2$-OPdG) (Figure 1).[7] Comparison of the *in vitro* replication of the ring-closed and ring-opened adducts by the Klenow fragment (exonuclease deficient) of DNA polymerase I ($Kf^-$) has demonstrated insertion of dT opposite $M_1dG$ and dC opposite $N^2$-OPdG, indicating $M_1dG$ has greater miscoding potential than $N^2$-OPdG.[8] These results predict that ring-opened adducts, such as OPdA, may be less miscoding than exocyclic adducts such as $M_1dG$. To test this hypothesis and ascertain potential contributions to mutagenesis in cells, we have analyzed the ability of polymerases from different subfamilies to perform translesion synthesis on templates containing OPdA.

We first employed several members of the Y-family of translesion polymerases. These enzymes play a critical role in the tolerance of DNA damage, but their low fidelity and efficiency have the potential to induce mutations within the

**Received:** August 13, 2013
**Revised:** October 25, 2013
**Published:** October 30, 2013

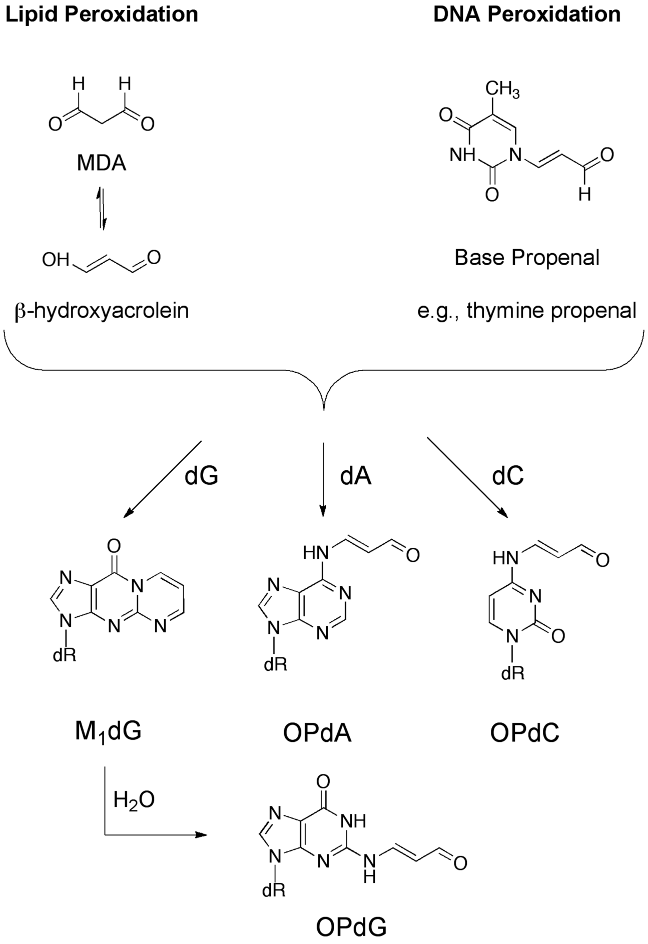

**Figure 1.** DNA damage from lipid and DNA peroxidation.

genome.[9,10] Furthermore, the induction of A → G transitions in *Escherichia coli* on replication of MDA-modified M13MB102 absolutely requires induction of the SOS response, suggesting the importance of error-prone polymerases such as *E. coli* Pol IV or Pol V in the mutagenic response.[11] Five translesion bypass polymerases have been identified in humans, four belonging to the Y-family of DNA polymerases (hPol $\eta$, hPol $\iota$, hPol $\kappa$, and Rev1[12,13]) and the fifth (hPol $\zeta$) belonging to the polymerase B-family.[14] Recent reports have shown that hPol $\theta$ also has lesion bypass properties.[15] For our analyses, we employed hPol $\eta$, hPol $\iota$, and hPol $\kappa$. In addition to translesion polymerases, we examined the bypass efficiency of two repair polymerases, Kf$^-$ and hPol $\beta$, and two replicative polymerases, the bacteriophage T7 DNA polymerase and Dpo1, a B-family polymerase from *Sulfolobus solfataricus*.

As the chemical instability of OPdA would complicate its *in vivo* mutagenic potential by site-specific methods, we explored its induction of mutations using *in vitro* approaches. To this end, we developed a postoligomerization route for the introduction of oxopropenyl adducts in DNA and used it to prepare a template containing OPdA at a defined position.[16] We then used this synthetic template to determine the ability of human translesion polymerases to bypass the OPdA adduct, as well as to quantify their bypass fidelity. Our studies reveal that human Y-family polymerases are able to correctly insert dTTP opposite OPdA. However, the frequency of insertion of dTTP opposite OPdA was reduced compared to the frequency of insertion of dTTP opposite unmodified dA. The effect on nontranslesion polymerases was also examined, and OPdA was found to significantly reduce T7 DNA polymerase activity and to completely block catalysis by hPol $\beta$. These results support the hypothesis that the ring-opened DNA adducts, such as OPdA, are likely to be less mutagenic than ring-closed adducts, although they can decrease and/or completely block polymerase activity.

## ■ MATERIALS AND METHODS

**Materials.** Recombinant hPol $\eta$ (amino acids 1−437), full-length hPol $\kappa$, and the catalytic core of hPol $\kappa$ (amino acids 19−526) were purified as described previously.[17−19] hPol $\beta$ was a kind gift from S. Wilson (National Institute of Environmental Health Sciences, Research Triangle Park, NC) and was purified as previously described.[20] This enzyme displayed a specific activity of ∼600 units/mg of protein, where 1 unit is the amount of enzyme required to catalyze the incorporation of 1 nmol of dTMP in 1 min at 20 °C using poly(dA)/oligo$(dT)_{20}$ as a template-primer.[20] The catalytic fragment of hPol $\iota$ (amino acids 1−420) was purified as described previously.[21] Klenow fragment exonuclease minus (Kf$^-$),[22] bacteriophage T7 DNA polymerase exonuclease minus (exo$^-$),[23] and *E. coli* thioredoxin[24] were expressed and purified as described previously. Exonuclease deficient *S. solfataricus* Dpo1 (exo$^-$) was expressed and purified as described previously.[25] [$\gamma$-$^{32}$P]ATP was obtained from Perkin-Elmer. T4 polynucleotide kinase and ultrapure grade solutions of dNTPs were purchased from New England Biolabs (Beverly, MA). Unmodified oligonucleotides were synthesized and purified by high-performance liquid chromatography (HPLC) in the Vanderbilt DNA Core (Nashville, TN). The OPdA-containing template oligonucleotide was synthesized by a postoligomerization modification strategy as described previously.[16] The 21-mer template sequence was 5′-TATCATGTCTGXTATCCCGGT-3′, where X was dA or OPdA. For assays measuring insertion of bases opposite the lesion, the 9-mer primer 5′-ACCGGGATA-3′ was used. For assays measuring the ability of polymerases to extend past the lesion, two 10-mer primers, 5′-ACCGGGATAT-3′ and 5′-ACCGGGATAC-3′, were used.

**HPLC Analysis of Oligonucleotides.** Oligonucleotides were analyzed on a Waters 2996 HPLC system with a photodiode array UV detector using a Phenomenex Polar-RP 80 Å, 4 $\mu$m C18 column (150 mm × 2.00 mm). Separation was achieved using a flow rate of 0.6 mL/min with the following mobile phases: A, which consisted of 95% (v/v) 0.1 M TEAA [triethylammonium acetate (pH 7.4)] and 5% (v/v) ACN, and B, which consisted of 74% (v/v) 0.1 M TEAA, 13% (v/v) ACN, and 13% (v/v) MeOH. Elution began at 0% B followed by a 40 min linear gradient to 65% B, a 20 min isocratic period at 65% B, and a 1 min equilibration to restore the initial conditions.

**Mass Spectrometric Analysis of OPdA-Modified Oligonucleotides.** Unmodified and OPdA-modified oligonucleotides were digested at 37 °C for 3 h in 17 mM sodium succinate, 8 mM $CaCl_2$, 2 mM $ZnSO_4$, and 50 mM MOPS (pH 6.0) with 4 × $10^3$ gel units of micrococcal nuclease (New England Biolabs) and 1.6 × $10^{-3}$ units of snake venom phosphodiesterase (Sigma). Following this incubation, 5 units of Antarctic Phosphatase (New England Biolabs) with 50 mM BIS-TRIS propane, 1 mM $MgCl_2$, and 0.1 mM $ZnCl_2$ (pH 6.0) was added, and reaction mixtures were incubated at 37 °C overnight. Following incubation, samples were spun through 3 kDa molecular mass cutoff filters (Millipore) to remove digestion enzymes. Samples were then dried under nitrogen and resuspended in 50 μL of HPLC grade water (Fisher Scientific). Liquid chromatography−tandem mass spectrometry (LC−MS/MS) analysis of samples was performed on a Thermo Surveyor autosampler and MS pump in-line with a Thermo Quantum triple-quadrupole mass spectrometer (Thermo Fisher Scientific). The mass spectrometer was equipped with an electrospray source and operated in positive ion mode. The analytes were chromatographed on the following reverse-phase gradient system: 5 to 60% B over 4 min, held at 60% B for 0.75 min, and returned to 5% B from 4.75 to 5 min. The column was then re-equilibrated at 5% B from 5 to 8 min. Mobile phase A consisted of $H_2O$ and 0.1% formic acid (v/v), and mobile phase B consisted of a 2:1 MeOH/ACN mixture and 0.03% (v/v) $HCO_2H$. The flow rate was 300 μL/min. A Phenomenex Polar-RP column [5.0 cm × 0.20 cm, 3 μm (Phenomenex, Torrence, CA)] was used at 25 °C. Following chromatographic separation and injection into the mass spectrometer, OPdA was detected with selected reaction monitoring with the following transition, $m/z$ 306 → 190, corresponding to the cleavage of the glycosidic bond and neutral loss of the deoxyribose moiety (−116 Da), with the positive charge remaining on the base. Neutral loss scans were performed with the same chromatographic separation of analytes and mass spectrometric detection of ions. To analyze the neutral loss of 116 Da, data were acquired from $m/z$ 150 to 400, and a collision energy of 13 eV was applied to induce cleavage of the deoxyribose moiety, resulting in a 116 Da loss.

***In Vitro* Replication Assays.** The 9-mer primer (100 pmol) was 5′-$^{32}$P-end-labeled with 10 units of T4 polynucleotide kinase and [γ-$^{32}$P]ATP (>6000 Ci/mmol, 250 μCi) in 50 mM $NaP_i$ (pH 7.4), 10 mM $MgCl_2$, and 5 mM dithiothreitol (DTT) for 1 h at 37 °C. The labeled primer strand was annealed (1:1 molar ratio) to the 21-mer template strand containing either dA or OPdA in the presence of 40 mM NaCl at 95 °C for 3 min and then slowly cooled to room temperature. The standard DNA polymerase reactions for both unmodified or OPdA-containing substrates were performed at 37 °C in 20 μL of buffered solutions containing 50 mM $NaP_i$ (pH 7.4), 5 mM $MgCl_2$, 5 mM DTT, 100 μg/mL bovine serum albumin (BSA), 10% (w/v) glycerol, 50 nM DNA substrate, an individual dNTP or all four (dATP, dCTP, dGTP, and dTTP) at 500 μM, and 5 nM hPol η (amino acids 1−437), hPol κ (full-length), hPol ι (amino acids 1−420), T7 DNA polymerase (exo$^-$), Kf$^-$, Dpo1 (exo$^-$), or hPol β. Reactions were terminated by the addition of 36 μL of loading buffer [10 mM EDTA, 95% (w/v) formamide, 0.03% (w/v) bromophenol blue, and 0.03% (w/v) cyanol blue] to a 4 μL aliquot of the reaction mixture before resolving products on a 20% (w/v) polyacrylamide gel containing 7 M urea. The radioactive products were then visualized using a Phosphorimager (Bio-Rad) equipped with Quantity One software for quantification. The percentage of extension was determined by comparing total extension products to unextended primer using the following relation: (intensity of extension products/total radioactivity in well) × 100. To quantify the full-length 21-mer product, densitometry was performed on the final 21-mer product following T7 (exo$^-$) polymerase extension and applied to the following relation: (intensity of final 21-mer)/(final 21-mer + 9-mer) × 100.

**Analysis of Steady-State Kinetics.** Steady-state kinetic reactions were performed in 50 mM $NaP_i$ buffer (pH 7.5) containing 5 mM DTT, 5 mM $MgCl_2$, 100 μg/mL BSA, 5% glycerol, 50 nM annealed 5′-$^{32}$P-end-labeled duplex DNA primer-template, 5 nM polymerase [hPol η (amino acids 1−437), hPol κ (amino acids 19−526), or hPol ι (amino acids 1−420)], and varying concentrations of individual dNTPs (0−800 μM). For both unadducted and OPdA-adducted substrates, samples were incubated at 25 °C for specified time intervals (0−190 min). Reactions were terminated by addition of 36 μL of loading buffer (96% formamide, 20 mM EDTA, bromophenol blue, and xylene cyanol), and products were separated on a 20% polyacrylamide (w/v)−7 M urea gel. The intensity of each gel band was quantified using a Phosphorimager (Bio-Rad) equipped with Quantity One software for quantification. The means and standard errors were determined from three individual experiments. Estimates for the turnover numbers ($k_{cat}$) and Michaelis constant ($K_{M,dNTP}$) were obtained by fitting the data to the Michaelis−Menten equation, using nonlinear regression curves [one-site hyperbolic fits in GraphPad Prism (GraphPad, San Diego, CA)].

## ■ RESULTS

**Synthesis and Characterization of OPdA-Containing Oligonucleotides.** To examine the impact of OPdA on polymerase activity, we synthesized and characterized a template oligonucleotide containing this lesion. Synthesis was performed using a postoligomerization modification strategy, resulting in the addition of one OPdA lesion at position 12 within the 21-mer (sequence in Materials and Methods).[16] A control template containing dA at position 12 was also synthesized. Characterization of the synthesized oligonucleotides by HPLC revealed that the unmodified and OPdA-modified templates eluted at 29 and 32 min, respectively (Figure 2). The purity of the OPdA-modified oligonucleotide was estimated to be ∼95% as evidenced by its chromatographic profile (Figure 2B). The OPdA-modified oligonucleotide exhibited an absorbance at 320 nm, characteristic of oxopropenyl amine chromophores (Figure 2C).[26] To confirm the presence of OPdA, both unmodified and OPdA-modified oligonucleotides were digested and analyzed using LC−MS/MS. The LC−MS/MS method utilized selected reaction monitoring to analyze the transition from $m/z$ 306 to 190, which corresponds to the OPdA precursor ($m/z$ 306) and the loss of deoxyribose (−116 Da to yield a product of $m/z$ 190). The chromatographic profiles of ions that contain the transition from $m/z$ 306 to 190 are displayed in Figure 3A. The top panel corresponds to a synthetic OPdA standard and displays a retention time of 3.2 min. The middle panel is the digested unmodified template, which does not display a peak at 3.2 min, indicating no OPdA is present in this sample. The bottom panel corresponds to the digested OPdA-modified template and a peak with a retention time of 3.2 min, indicating the presence of OPdA in this sample. Further confirmation of the presence of OPdA in the synthetic oligonucleotide was achieved by employing neutral loss mass spectrometric examination of digested unmodified and OPdA-modified templates, which monitored the loss of 116 Da (deoxyribose) (Figure 3B,C). This analysis results in the identification of precursor ions that lose 116 Da following application of a collision energy of 13 eV. Analysis of ions present in the digested unmodified oligonucleotide sample that elute between 0.5 and 4 min revealed four major ions, which corresponded to dA, dC, dG, and dT (Figure 3B). Similarly, the examination of ions in the digested OPdA-modified oligonucleotide sample that elute between 0.5 and 4 min displayed precursor ions that

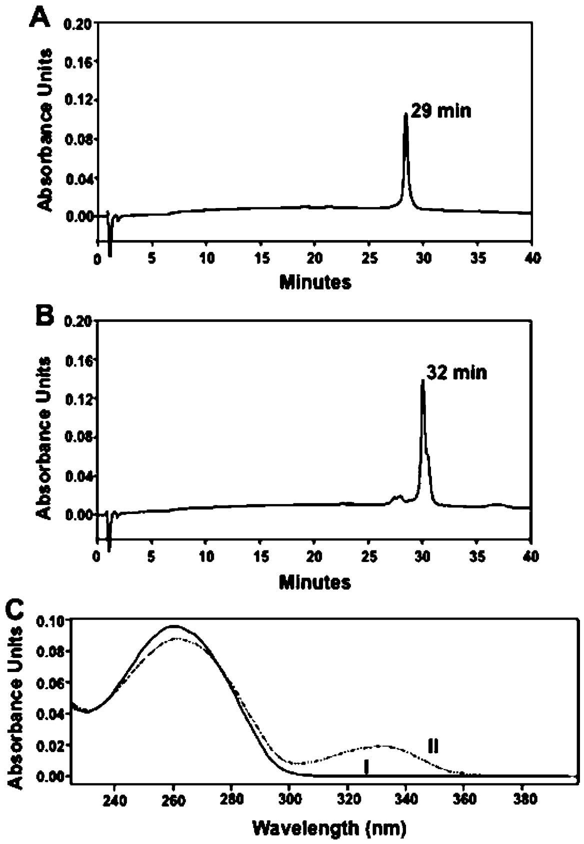

**Figure 2.** HPLC analysis of OPdA-modified oligonucleotides. Oligonucleotides were analyzed by HPLC as described in Materials and Methods. (A) HPLC analysis of the unmodified 21-mer oligonucleotide (retention time of 29 min). (B) HPLC analysis of the OPdA-modified 21-mer oligonucleotide (retention time of 32 min). (C) Comparison of the UV spectra of unmodified and OPdA-modified 21-mer oligonucleotides. The solid line (spectrum I) corresponds to the unmodified 21-mer and the dashed line (spectrum II) to the OPdA-modified 21-mer. Sequences of oligonucleotides are listed in Materials and Methods.

corresponded to dA, dC, dG, and dT, but this sample also exhibited an ion that corresponded to OPdA (Figure 3C). These data confirm the presence of OPdA in the synthetically modified template.

**Examination of Translesion DNA Polymerase Activity past dA and OPdA.** Following confirmation of the presence of OPdA within the synthesized template, *in vitro* extension experiments were conducted to determine the effect of the lesion on DNA polymerase activity. These studies were initiated using the human translesion polymerases, hPol *η* (residues 1−437), hPol *κ* (full-length and catalytic core, residues 19−526), and hPol *ι* (residues 1−420), as their ability to bypass a range of DNA adducts makes them likely candidates for bypassing OPdA.[27,28] In addition, these polymerases are relatively error-prone and may be responsible for OPdA-induced mutations.[28]

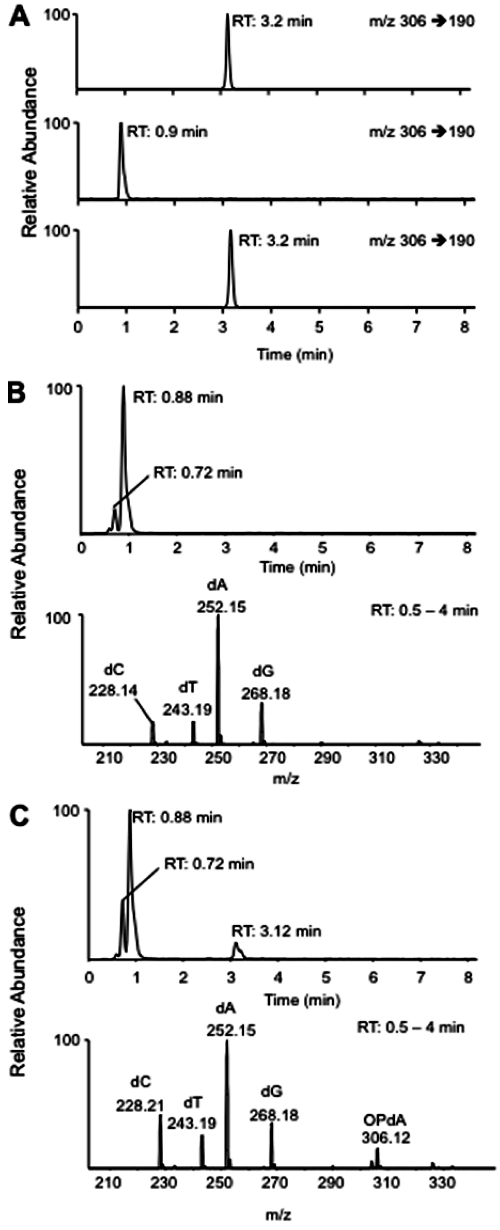

**Figure 3.** Mass spectrometric analysis of OPdA-modified oligonucleotides. Unmodified and OPdA-modified oligonucleotides were digested and analyzed using MS. (A) Selective reaction monitoring of the transition for OPdA (from *m*/*z* 306 to 190), representing the loss of deoxyribose, was employed. The top panel shows data for the OPdA standard, the middle panel data for the unmodified oligonucleotide, and the bottom panel data for the OPdA-modified oligonucleotide. (B) A neutral loss scan of unmodified oligonucleotide was performed as described in Materials and Methods. The top panel represents the reconstructed ion chromatogram, and the bottom panel demonstrates *m*/*z* ions present at retention times from 0.5 to 4 min. (C) Analysis of the OPdA-modified oligonucleotide as described for panel B.

To analyze polymerase extension past OPdA, a 9-mer primer was annealed to either the unmodified 21-mer control template or the OPdA-modified template, and the resulting substrates were incubated with one of the translesion polymerases in the presence of all four dNTPs. As seen in Figure 4A, human Pol *η* (residues 1−437) (termed hPol *η* throughout) extended the primer completely to the terminus of the oligonucleotide and, by 15 min, displayed no obvious difference in the bypass of dA compared to that of OPdA. However, a slight decrease in the degree of extension across OPdA at the shortest time point (5 min) prompted analysis of the degree of extension over a shorter time frame (0.25−5 min), which revealed a reduced level of polymerase action opposite OPdA (Figure 4B). Similar to hPol *η*, full-length hPol *κ* was found to bypass the OPdA lesion to produce an extension product of 21 bases, and a slight

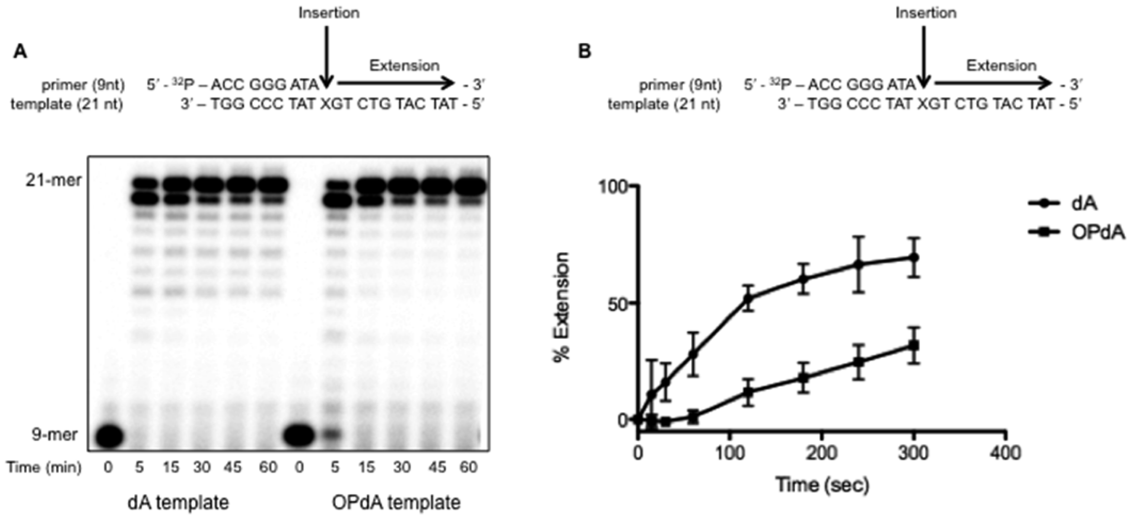

**Figure 4.** Primer extension by hPol $\eta$ opposite dA and OPdA. (A) hPol $\eta$ (5 nM) was incubated in the presence of either unmodified or OPdA-modified 9/21-mer radiolabeled substrate (50 nM) and four dNTPs (500 $\mu$M) as described in Materials and Methods. Reactions were performed over increasing amounts of incubation time as indicated. The quenched (EDTA) samples were analyzed by 20% (w/v) denaturing polyacrylamide gel electrophoresis, and the amount of product formed was visualized using a phosphorimager. (B) Reactions were performed as described for panel A on a shorter time course. Data were quantified as described in Materials and Methods and represent the average of three independent experiments.

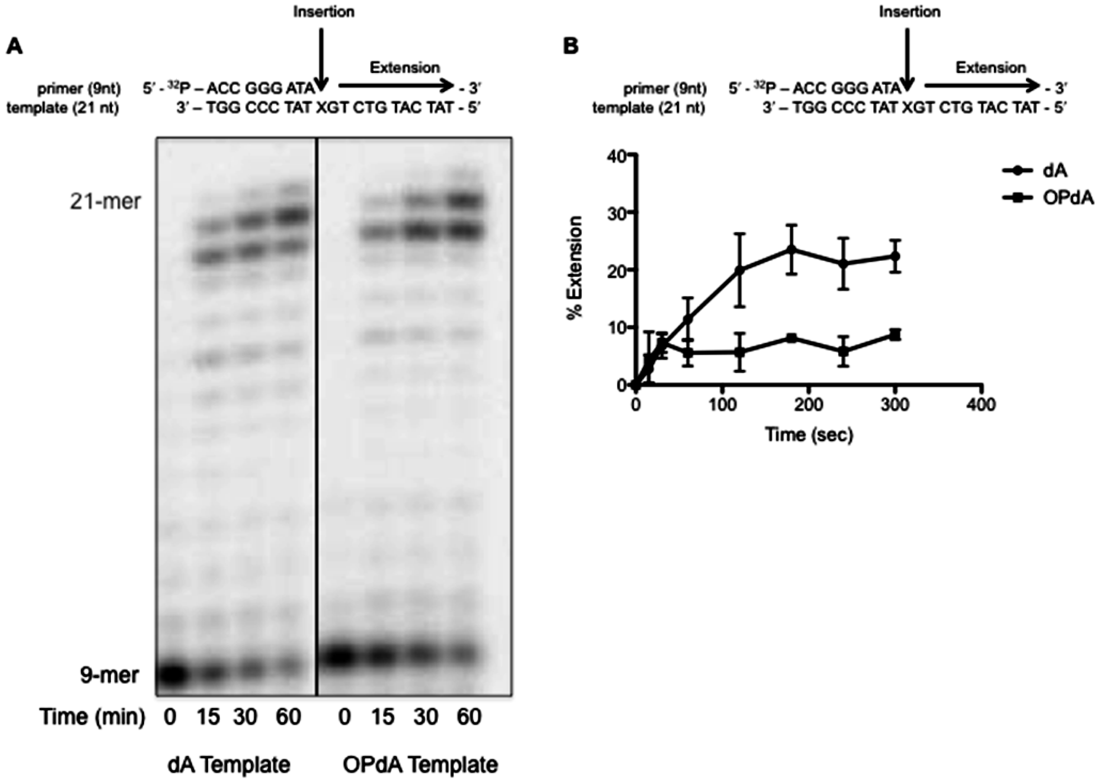

**Figure 5.** Primer extension by hPol $\kappa$ opposite dA and OPdA. (A) hPol $\kappa$ (5 nM) was incubated in the presence of either unmodified or OPdA modified 9/21-mer radiolabeled substrate (50 nM) and four dNTPs (500 $\mu$M) as described in Materials and Methods. Reactions were performed over increasing amounts of incubation time as indicated. The quenched (EDTA) samples were analyzed by 20% (w/v) denaturing polyacrylamide gel electrophoresis, and the amount of product formed was visualized using a phosphorimager. (B) Reactions were performed as described for panel A on a shorter time course. Data were quantified as described in Materials and Methods and represent the average of three independent experiments.

decrease in the level of product formation at 5 min was also observed (Figure 5A). Shorter time course analysis revealed stalling of full-length hPol $\kappa$ and a decrease in polymerase activity upon extension past OPdA (Figure 5B).

The extremely low processivity of hPol $\iota$ (residues 1−420) (termed hPol $\iota$ throughout) has been demonstrated previously; extension is typically limited to one to three nucleotides.[29,30] Therefore, it was not surprising in this analysis that hPol $\iota$ generated a final extension product of only 13 bases upon replication past dA over a time course of 60 min (Figure 6). Extension of hPol $\iota$ past OPdA revealed an even shorter product of only 11 bases, consistent with insertion of a dNTP

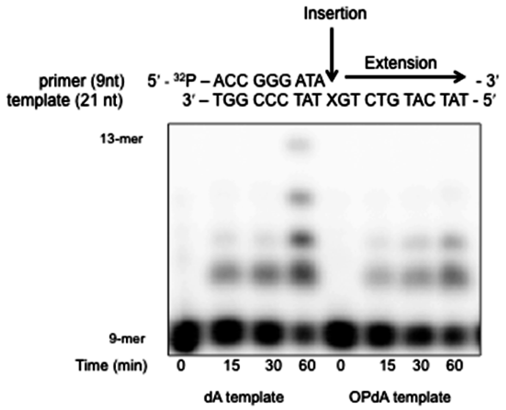

**Figure 6.** Primer extension by hPol ι opposite dA and OPdA. hPol ι (5 nM) was incubated in the presence of either unmodified or OPdA modified 9/21-mer radiolabeled substrate (50 nM) and four dNTPs (500 μM) as described in Materials and Methods. Reactions were performed over increasing amounts of incubation time as indicated. The quenched (EDTA) samples were analyzed by 20% (w/v) denaturing polyacrylamide gel electrophoresis, and the amount of product formed was visualized using a phosphorimager.

opposite OPdA followed by extension of a single dNTP (Figure 6).

**Steady-State Kinetic Analysis of Translesion DNA Polymerase Activity.** Although hPol η and full-length hPol κ were able to bypass OPdA with full primer extension, our preliminary results suggest that the lesion negatively impacts the catalytic efficiency of these enzymes. To more fully characterize this effect and to probe the potential of each enzyme for nucleotide mis-incorporation, we examined the kinetics of base insertion opposite OPdA. Steady-state kinetic analysis of the insertion of single nucleotides opposite OPdA and dA by each polymerase was performed utilizing 9-mer primers annealed to the appropriate 21-mer templates incubated in the presence of each dNTP individually under steady-state conditions. From the dNTP insertion kinetics, the $k_{cat}$ and $K_{M,dNTP}$ values were obtained by fitting the data to the Michaelis–Menten equation using nonlinear regression (Tables 1–3). This methodology allows a comparison of the catalytic efficiency ($k_{cat}/K_{M,dNTP}$) of insertion of a correct (dTTP) versus incorrect nucleotide opposite OPdA and dA, providing an assessment of mis-insertion frequency for each polymerase tested.

Examination of incorporation of a single nucleotide by hPol η revealed preferential insertion of dTTP opposite both dA and OPdA. The efficiency of incorporation of dTTP opposite OPdA was approximately 34% of that observed for template dA (Table 1). Incorrect base insertion by hPol η was also observed for both dA and OPdA. Interestingly, dATP was the primary mis-insertion event opposite dA, whereas dCTP was primarily mis-incorporated opposite OPdA (Table 1). The fidelity of hPol η is somewhat improved for OPdA-containing templates. Insertion of dTTP opposite dA is ∼56-fold more efficient than mis-insertion of dATP, whereas insertion of dTTP opposite OPdA is ∼230-fold better than the mis-insertion of dCTP.

For hPol κ (residues 19–526), the catalytic efficiency for insertion of dTTP opposite OPdA was approximately 26% of the efficiency for insertion of dTTP opposite dA (Table 2). This polymerase also inserted all four dNTPs opposite both dA and OPdA; however, hPol κ (residues 19–526) was found to be slightly more accurate than hPol η in the insertion of a nucleotide opposite OPdA (Table 2 compared to Table 1). Mis-insertion of dCTP opposite OPdA was the most frequent mis-insertion event, as was seen for hPol η (Table 2), but there was an ∼1000-fold preference for accurate insertion by hPol κ (residues 19–526), as opposed to an only ∼230-fold preference for accurate insertion by hPol η.

hPol ι catalyzed the formation of a two-nucleotide extension product when replicating past OPdA, which is typical for this very nonprocessive enzyme (Figure 6). The catalytic efficiency of insertion was approximately 29% of the efficiency observed for the insertion of dTTP opposite dA (Table 3). hPol ι was able to insert all four dNTPs opposite dA; however, only dTTP and dCTP were inserted opposite OPdA (Table 3). The specificity constant defining insertion of dTTP opposite OPdA by hPol ι was ∼36-fold greater than that for mis-insertion of dCTP.

In summary, although hPol η and full-length hPol κ extended the primer to the template terminus, the efficiency for insertion of the correct nucleotide opposite the lesion of hPol κ (residues 19–526) and hPol η is reduced ∼3-fold compared to that of dA. A similar reduction in catalytic efficiency was also observed for hPol ι, which was accompanied by truncated primer extension. All three Y-family polymerases preferentially incorporated the correct nucleotide (dTTP) opposite OPdA, with hPol κ (residues 19–526) displaying the greatest fidelity opposite the lesion and the highly error-prone hPol ι showing the least faithful copying of OPdA.

**Steady-State Kinetic Analysis of Next-Base Extension by Y-Family Human DNA Polymerases.** To examine polymerase extension past the OPdA lesion, 10-mer primers were synthesized to position dT opposite OPdA or dA. The template sequence contains a dG residue 5′ to OPdA or dA,

**Table 1. Steady-State Kinetic Parameters for Insertion of a Single Nucleotide by hPol η opposite dA and OPdA**[a]

| DNA substrate | incoming nucleotide | $k_{cat}$ (min$^{-1}$) | $K_{M,dNTP}$ (μM) | $k_{cat}/K_M$ (μM$^{-1}$ min$^{-1}$) | $f$ (relative insertion frequency) |
|---|---|---|---|---|---|
| insertion opposite dA | dTTP | 0.74 ± 0.03 | 1.4 ± 0.5 | 0.53 | 1 |
| 5′-ATA | dATP | 0.15 ± 0.01 | 16 ± 7 | $9.5 \times 10^{-3}$ | 0.019 |
| 3′-TATXGTCTG-5′ | dCTP | 0.03 ± 0.01 | 11 ± 9 | $3 \times 10^{-3}$ | 0.005 |
| X = dA | dGTP | 0.02 ± 0.01 | 10 ± 2 | $2 \times 10^{-3}$ | 0.004 |
| insertion opposite OPdA | dTTP | 0.62 ± 0.08 | 3.5 ± 2 | 0.18 | 0.34 |
| 5′-ATA | dATP | 0.005 ± 0.001 | 83 ± 73 | $6 \times 10^{-5}$ | 0.0001 |
| 3′-TATXGTCTG-5′ | dCTP | 0.015 ± 0.001 | 19 ± 12 | $7.9 \times 10^{-4}$ | 0.0015 |
| X = OPdA | dGTP | 0.007 ± 0.001 | 33 ± 22 | $2 \times 10^{-4}$ | 0.0004 |

[a] For determination of steady-state kinetic values, graphs of product formation vs dNTP concentration were plotted using nonlinear regression analysis (one-site hyperbolic fit) in GraphPad Prism. The mis-insertion frequencies were calculated relative to insertion of dTTP opposite control (dA) primer-templates as the ($k_{cat}/K_{M,dNTP}$)/($k_{cat}/K_{M,dTTP}$) ratio.

Table 2. Steady-State Kinetic Parameters for Insertion of a Single Nucleotide by hPol $\kappa$ opposite dA and OPdA[a]

| DNA substrate | incoming nucleotide | $k_{cat}$ (min$^{-1}$) | $K_{M,dNTP}$ ($\mu$M) | $k_{cat}/K_M$ ($\mu$M$^{-1}$ min$^{-1}$) | $f$ (relative insertion frequency) |
|---|---|---|---|---|---|
| insertion opposite dA | dTTP | 0.60 ± 0.06 | 0.4 ± 0.2 | 1.5 | 1 |
| 5′-ATA | dATP | 0.003 ± 0.001 | 11 ± 9 | $3 \times 10^{-4}$ | 0.0002 |
| 3′-TATXGTCTG-5′ | dCTP | 0.008 ± 0.001 | 33 ± 29 | $2 \times 10^{-4}$ | 0.0001 |
| X = dA | dGTP | 0.004 ± 0.001 | 6.5 ± 3.5 | $6. \times 10^{-4}$ | 0.0004 |
| insertion opposite OPdA | dTTP | 0.59 ± 0.06 | 1.5 ± 0.8 | 0.39 | 0.26 |
| 5′-ATA | dATP | 0.010 ± 0.004 | 15 ± 110 | $6.6 \times 10^{-5}$ | 0.00004 |
| 3′-TATXGTCTG-5′ | dCTP | 0.009 ± 0.001 | 23 ± 16 | $4 \times 10^{-4}$ | 0.0003 |
| X = OPdA | dGTP | 0.010 ± 0.002 | 58 ± 51 | $1.7 \times 10^{-4}$ | 0.00011 |

[a] For determination of steady-state kinetic values, graphs of product formation vs dNTP concentration were plotted using nonlinear regression analysis (one-site hyperbolic fit) in GraphPad Prism. The mis-insertion frequencies were calculated relative to insertion of dTTP opposite control (dA) primer-templates as the $(k_{cat}/K_{M,dNTP})/(k_{cat}/K_{M,dTTP})$ ratio.

Table 3. Steady-State Kinetic Parameters for Insertion of a Single Nucleotide by hPol $\iota$ opposite dA and OPdA[a]

| DNA substrate | incoming nucleotide | $k_{cat}$ (min$^{-1}$) | $K_{M,dNTP}$ ($\mu$M) | $k_{cat}/K_M$ ($\mu$M$^{-1}$ min$^{-1}$) | $f$ (relative insertion frequency) |
|---|---|---|---|---|---|
| insertion opposite dA | dTTP | 0.66 ± 0.06 | 7.0 ± 3.0 | 0.094 | 1 |
| 5′-ATA | dATP | 0.060 ± 0.008 | 190 ± 70 | $3.2 \times 10^{-4}$ | 0.0034 |
| 3′-TATXGTCTG-5′ | dCTP | 0.020 ± 0.002 | 180 ± 50 | $1.1 \times 10^{-4}$ | 0.0012 |
| X = dA | dGTP | 0.010 ± 0.003 | 150 ± 80 | $6.7 \times 10^{-5}$ | 0.00071 |
| insertion opposite OPdA | dTTP | 0.60 ± 0.09 | 22 ± 19 | 0.027 | 0.29 |
| 5′-ATA | dATP | – | – | – | – |
| 3′-TATXGTCTG-5′ | dCTP | 0.070 ± 0.010 | 94 ± 40 | $7.4 \times 10^{-4}$ | 0.0079 |
| X = OPdA | dGTP | – | – | – | – |

[a] For determination of steady-state kinetic values, graphs of product formation vs dNTP concentration were plotted using nonlinear regression analysis (one-site hyperbolic fit) in GraphPad Prism. The mis-insertion frequencies were calculated relative to insertion of dTTP opposite control (dA) primer-templates as the $(k_{cat}/K_{M,dNTP})/(k_{cat}/K_{M,dTTP})$ ratio.

Table 4. Steady-State Kinetic Parameters for Next-Base Extension by hPol $\eta$ past dA and OPdA[a]

| incoming nucleotide | DNA substrate | $k_{cat}$ (min$^{-1}$) | $K_{M,dNTP}$ ($\mu$M) | $k_{cat}/K_M$ ($\mu$M$^{-1}$ min$^{-1}$) | $f$ (relative insertion frequency) |
|---|---|---|---|---|---|
| dCTP:dG | dT:dA | 0.66 ± 0.01 | 0.30 ± 0.08 | 2.2 | 1 |
| | dC:dA | 0.070 ± 0.002 | 0.40 ± 0.1 | 0.18 | 0.080 |
| dCTP:dG | dT:OPdA | 0.40 ± 0.09 | 12 ± 8 | 0.033 | 0.015 |
| | dC:OPdA | 0.02 ± 0.01 | 0.8 ± 0.6 | 0.02 | 0.01 |

[a] For determination of steady-state kinetic values, graphs of product formation vs dNTP concentration were plotted using nonlinear regression analysis (one-site hyperbolic fit) in GraphPad Prism. The mis-insertion frequencies were calculated relative to insertion of dTTP opposite control (dA) primer-templates as the $(k_{cat}/K_{M,dNTP})/(k_{cat}/K_{M,dCTP})$ ratio.

Table 5. Steady-State Kinetic Parameters for Next-Base Extension by hPol $\iota$ past dA and OPdA[a]

| incoming nucleotide | DNA substrate | $k_{cat}$ (min$^{-1}$) | $K_{M,dNTP}$ ($\mu$M) | $k_{cat}/K_M$ ($\mu$M$^{-1}$ min$^{-1}$) | $f$ (relative insertion frequency) |
|---|---|---|---|---|---|
| dCTP:dG | dT:dA | 0.56 ± 0.02 | 13 ± 3 | 0.043 | 1 |
| | dC:dA | – | – | – | – |
| dCTP:dG | dT:OPdA | 0.33 ± 0.05 | 11 ± 8 | 0.030 | 0.70 |
| | dC:OPdA | – | – | – | – |

[a] For determination of steady-state kinetic values, graphs of product formation vs dNTP concentration were plotted using nonlinear regression analysis (one-site hyperbolic fit) in GraphPad Prism. The mis-insertion frequencies were calculated relative to insertion of dTTP opposite control (dA) primer-templates as the $(k_{cat}/K_{M,dNTP})/(k_{cat}/K_{M,dCTP})$ ratio.

Table 6. Steady-State Kinetic Parameters for Next-Base Extension by hPol $\kappa$ past dA and OPdA[a]

| incoming nucleotide | DNA substrate | $k_{cat}$ (min$^{-1}$) | $K_{M,dNTP}$ ($\mu$M) | $k_{cat}/K_M$ ($\mu$M$^{-1}$ min$^{-1}$) | $f$ (relative insertion frequency) |
|---|---|---|---|---|---|
| dCTP:dG | dT:dA | 1.3 ± 0.1 | 3.0 ± 1.0 | 0.43 | 1 |
| | dC:dA | 0.80 ± 0.09 | 5.6 ± 2.9 | 0.14 | 0.33 |
| dCTP:dG | dT:OPdA | 1.3 ± 0.1 | 1.7 ± 0.8 | 0.76 | 1.8 |
| | dC:OPdA | 0.05 ± 0.01 | 10 ± 7 | 0.005 | 0.01 |

[a] For determination of steady-state kinetic values, graphs of product formation vs dNTP concentration were plotted using nonlinear regression analysis (one-site hyperbolic fit) in GraphPad Prism. The mis-insertion frequencies were calculated relative to insertion of dTTP opposite control (dA) primer-templates as the $(k_{cat}/K_{M,dNTP})/(k_{cat}/K_{M,dCTP})$ ratio.

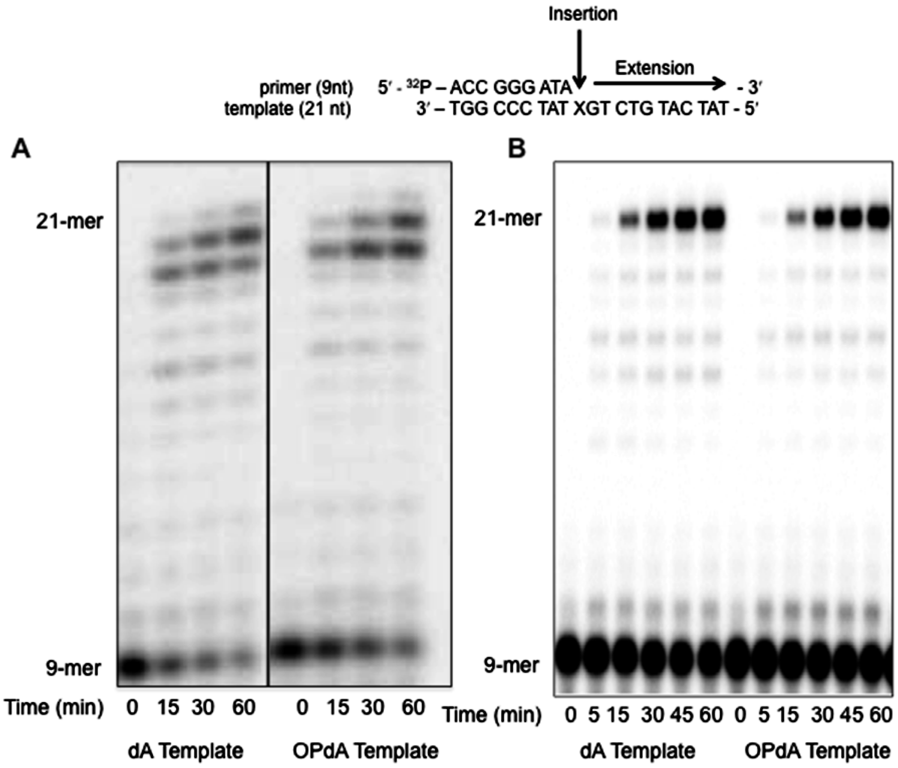

**Figure 7.** Primer extension by Kf$^-$ and Dpo1 (exo$^-$) opposite dA and OPdA. (A) Kf$^-$ (5 nM) was incubated in the presence of either unmodified or OPdA-modified 9/21-mer radiolabeled substrate (50 nM) and four dNTPs (500 $\mu$M) as described in Materials and Methods. Reactions were performed over increasing amounts of incubation time as indicated. The quenched (EDTA) samples were analyzed by 20% (w/v) denaturing polyacrylamide gel electrophoresis, and the amount of product formed was visualized using a phosphorimager. (B) Extension experiments were performed with Dpo1 (exo$^-$) (5 nM) as described for panel A.

presenting this base as the next available template base for polymerase insertion. The annealed product was then incubated with dCTP to determine rates of insertion from the dA:dT or OPdA:dT base pair. Analysis of hPol $\eta$-catalyzed extension past the lesion displayed a dramatic reduction (98%) in efficiency with the dT:OPdA base pair compared to that with the dT:dA base pair substrate (Table 4). hPol $\iota$ also displayed a reduced efficiency of extension (30%) of the dT:OPdA base pair as compared to the dT:dA base pair (Table 5). In contrast, hPol $\kappa$ (residues 19–526) displayed a 1.8-fold increase in the efficiency of insertion of dCTP opposite dG upon extension from the dT:OPdA base pair as compared to dT:dA (Table 6).

Because dCTP was the base primarily mis-inserted opposite OPdA, the ability of polymerases to extend past a dC mismatch (dC:dA or dC:OPdA) was also investigated. The extension efficiency of hPol $\eta$ was reduced when either the dC:dA or dC:OPdA base pair was present (92 or 99% decreased efficiency, respectively, compared to that with dT:dA) (Table 4). These mismatches also decreased the extension efficiency of hPol $\kappa$ (residues 19–526), with 67 and 99% reduced levels of extension for dC:dA and dC:OPdA mismatches, respectively, compared to that for dT:dA (Table 6). hPol $\iota$ was unable to extend the dCTP:dA or dCTP:OPdA mispair (Table 5).

**Analysis of Nontranslesion DNA Polymerase-Catalyzed Extension past OPdA.** As described above, translesion DNA polymerases exhibit a modest overall decrease in the catalytic efficiency of insertion of dTTP opposite OPdA as compared to dA, and OPdA decreased the final extension length of primers extended by hPol $\iota$ (Figures 4–6 and Tables 1–3). The effect of OPdA upon mis-insertion frequency was variable for the three Y-family polymerases, with hPol $\eta$ displaying a slightly increased fidelity opposite OPdA when compared to dA and hPol $\iota$ and hPol $\kappa$ (residues 19–526) losing some ability in selecting the correct nucleotide during insertion opposite OPdA. However, all of the Y-family polymerases preferred insertion of dTTP opposite OPdA, and though it lost some accuracy relative to template dA, hPol $\kappa$ (residues 19–526) actually exhibited the strongest ability to select dTTP over mispairs when catalyzing insertion opposite OPdA, preferring dTTP ~1000-fold over dCTP. To determine the specificity of these effects for translesion polymerases, we next investigated the impact of OPdA on the activity of nontranslesion polymerase (i.e., processive) DNA polymerases.

The ability of other polymerase families to bypass OPdA was examined using the same template primers and experimental conditions employed for the study of Y-family polymerases. The model A-family polymerase, Kf$^-$, was found to completely extend the primer to the final oligonucleotide length of 21 bases with essentially the same efficiency regardless of the presence of dA or OPdA (Figure 7A). These results indicate that OPdA impacts Kf$^-$ activity in a manner similar to that observed previously for $N^2$-OPdG, demonstrating that ring-opened DNA adducts do not act as a block to Kf$^-$ activity. It is worth noting that the ring-closed form of $N^2$-OPdG, $M_1$dG, blocks Kf$^-$ activity.[8]

We also examined the impact of OPdA on the B-family polymerase Dpo1 (exo$^-$) from *S. solifataricus*. Like the results for Kf$^-$, OPdA only minimally perturbed Dpo1 (exo$^-$) polymerase extension activity (Figure 7B). We next examined a model C-family member, the bacteriophage replicative T7

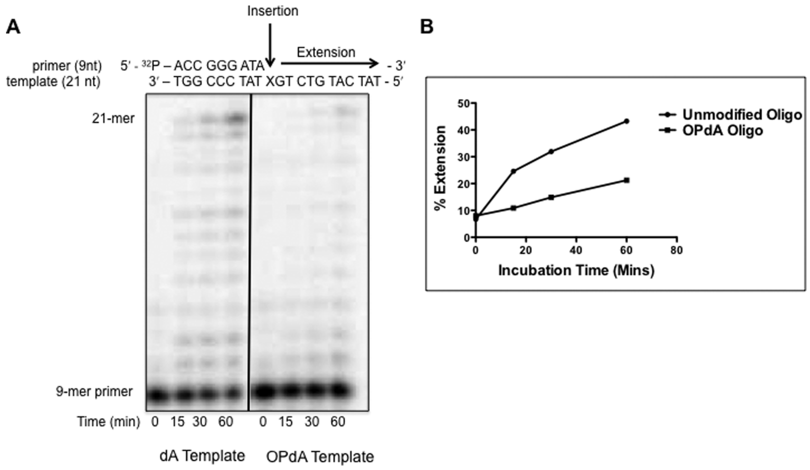

**Figure 8.** Primer extension by T7 (exo$^-$) polymerase opposite dA and OPdA. (A) T7 polymerase (exo$^-$) (5 nM) was incubated in the presence of either unmodified or OPdA-modified 9/21-mer radiolabeled substrate (50 nM) and four dNTPs (500 μM) as described in Materials and Methods. Reactions were performed with increasing amounts of incubation time as indicated. The quenched (EDTA) samples were analyzed by 20% (w/v) denaturing polyacrylamide gel electrophoresis, and the amount of product formed was visualized using a phosphorimager. (B) Quantitation of three replicate extension experiments, a representation of which can be seen in panel A.

(exo$^-$) DNA polymerase. Interestingly, OPdA dramatically decreased the activity of this polymerase compared to its activity on unmodified DNA (Figure 8). The reduction in T7 (exo$^-$) polymerase activity prompted us to investigate an additional polymerase, hPol β, which is an X-family member involved in base excision repair. Surprisingly, this polymerase displayed a nearly complete lack of activity on an OPdA-containing template-primer (Figure 9).

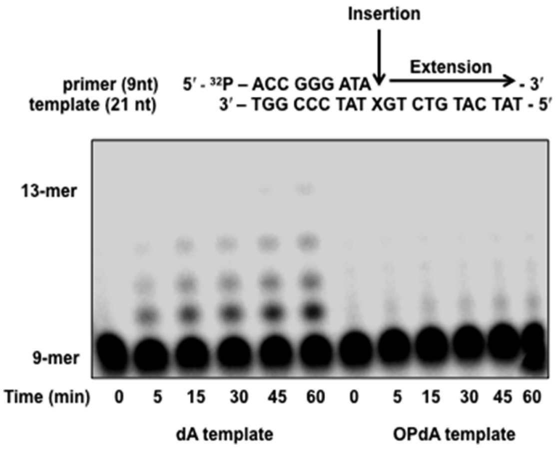

**Figure 9.** Primer extension by hPol β opposite dA and OPdA. hPol β (5 nM) was incubated in the presence of either unmodified or OPdA modified 9–21-mer radiolabeled substrate (50 nM) and four dNTPs (500 μM) as described in Materials and Methods. Reactions were performed with increasing amounts of incubation time as indicated. The quenched (EDTA) samples were analyzed by 20% (w/v) denaturing polyacrylamide gel electrophoresis, and the amount of product formed was visualized using a phosphorimager.

## ■ DISCUSSION

These studies demonstrate that OPdA only modestly decreases the efficiency of the translesion polymerases hPol η, hPol κ (full-length and residues 19–526), and hPol ι as well as Dpo1 (exo$^-$) and Kf$^-$, with stronger inhibition observed for the replicative bacteriophage T7 (exo$^-$) polymerase and the X-family member hPol β. hPol η, hPol κ, and T7 (exo$^-$) polymerase fully extended the primer to the template terminus; however, the efficiency of this extension was most noticeably decreased for T7 (exo$^-$). hPol ι extended the primer three or four nucleotides when replicating past dA, but primer extension past OPdA was limited to two nucleotides. Strikingly, the activity of repair polymerase hPol β was nearly completely blocked by the presence of OPdA.

It is interesting to compare the decrease in translesion polymerase activity on OPdA-containing templates to previous results with the exocyclic $M_1dG$ adduct.[28] Previously, we found that the efficiency of nucleotide insertion ($k_{cat}/K_M$) by hPol κ (residues 19–526) was reduced ~30-fold for insertion of dCTP opposite $M_1dG$, an impact larger than that observed for insertion opposite OPdA compared to dA (4-fold).[28] The reduction in hPol ι insertion frequency opposite $M_1dG$ compared to dG (10- or 25-fold, depending on the sequence context) was also greater than that observed for OPdA opposite dA (3-fold).[28] Overall, these results indicate that, although both adducts hinder polymerase activity, $M_1dG$ decreases polymerase activity to a greater extent than OPdA. This finding is consistent with the hypothesis that the exocyclic $M_1dG$ adduct exerts a larger disruption to replication than ring-opened adducts such as OPdA.

Changes in the specificity constants describing Y-family polymerase activity on OPdA-containing substrates are primarily driven by higher $K_{M,dNTP}$ values. The $k_{cat}$ for insertion of dTTP opposite OPdA remains largely unchanged relative to that for dA for all three Y-family members. Examination of the $K_{M,dNTP}$ for the insertion of the correct base, dTTP, opposite OPdA revealed 3.5-, 3-, and 4-fold increases compared to insertion opposite dA for hPol η, hPol ι, and hPol κ (residues 19–526), respectively. The increase in $K_{M,dNTP}$ suggests these polymerases require higher concentrations of dTTP to form productive complexes when bypassing OPdA, which then manifests as a decreased specificity constant. Comparatively, insertion of dCTP opposite $M_1dG$ revealed a 5–10-fold increase in $K_{M,dNTP}$ (depending on the sequence context).[28]

Extension of the primer following insertion of a base opposite OPdA was examined by analysis of insertion of dCTP opposite dG located adjacent to an OPdA:dT or dA:dT base pair. Both hPol $\eta$ and hPol $\iota$ displayed reduced efficiencies of insertion of dCTP opposite dG from an OPdA:dT base pair compared to a dA:dT base pair, exhibiting 100- and 1.4-fold reduced insertion efficiencies, respectively. Interestingly, hPol $\kappa$ displayed a 1.8-fold increase in next-base extension activity compared to extension from dA. From these data, hPol $\kappa$ (residues 19−526) is the most effective polymerase in extending from the base-paired OPdA lesion and hPol $\eta$ is very inefficient, and hPol $\iota$ is slightly inhibited compared to extension from a dA:dT base pair. These data are consistent with previously published analysis of the catalytic core enzymes.

Although the examined translesion polymerases primarily insert the correct base (dTTP) opposite OPdA, dCTP was inserted second most frequently. This insertion event was several hundred-fold less efficient than insertion of dTTP, suggesting a low mutagenic potential for OPdA. Among the translesion polymerases tested, hPol $\iota$ is the most error-prone but extends the primer fully following base insertion. Conversely, hPol $\kappa$ (residues 19−526) performs more accurate bypass of OPdA, and full-length hPol $\kappa$ efficiently extends the primer. hPol $\iota$ is also error-prone and is unable to fully extend the primer to the terminus following base insertion. Insertion of dCTP opposite OPdA would generate A → G transitions in the second round of replication, consistent with our previous speculation that adenine adducts may be responsible for generating A → G transitions that contribute to overall MDA mutagenicity in *E. coli*.[11]

As our data demonstrate the minimal mutagenic potential of OPdA, we sought to compare this to the mutagenicity of other DNA adducts. Analysis of full-length hPol $\kappa$ replication across a variety of $N^2$-guanyl adducts revealed varying degrees of mis-insertions, which were generally ∼100-fold less likely to occur than correct base insertion, comparable to the mis-insertion frequency observed for OPdA.[18] Examination of the mis-insertion frequency of $M_1dG$ demonstrates a 5−20-fold reduction in insertion frequency compared to that of dCTP, depending on the sequence context and the base being inserted.[28] Mis-incorporation of bases opposite $M_1dG$ occurs much more frequently than mis-insertion events observed opposite OPdA, supporting our hypothesis that ring-opened adducts such as OPdA are less mutagenic than the bulkier, exocyclic adduct $M_1dG$.

We expanded our investigation to determine the ability of nontranslesion polymerases to replicate past OPdA. These analyses revealed a decrease in T7 (exo$^-$) polymerase activity and a substantial block of hPol $\beta$ activity with a minimal effect on Kf$^-$ or Dpo1 (exo$^-$) polymerase activity. Guanine-modified DNA adducts, including 8-oxo-G, $O^6$-methylG, and $O^6$-benzylG, have been shown to influence T7 (exo$^-$) polymerase activity, leading to error-prone bypass and a decrease in polymerase efficiency.[24,31] Interestingly, T7 (exo$^-$) polymerase can efficiently bypass $N^2$-methylG, but it is strongly blocked by $N^2$-ethylG and $N^2$-benzylG.[32] The very substantial inhibition of hPol $\beta$ activity was interesting considering this polymerase has been shown to efficiently bypass bulky cisplatin-induced DNA adducts.[33] Additionally, hPol $\beta$ induces both substitutions and frameshift mutations when replicating past propanodeoxyguanosine.[34] OPdA, therefore, acts in a unique manner to block hPol $\beta$ replication.

This study represents the first characterization of the impact of OPdA on DNA replication. The results suggest that bypass of OPdA will be slightly error-prone when the adduct is replicated by Y-family polymerase, but to a much lesser extent than $M_1dG$. hPol $\eta$ is the least perturbed Y-family polymerase, while hPol $\kappa$ (residues 19−526) is the most accurate during insertion opposite OPdA and the most efficient at extending from the dT:OPdA base pair. These results suggest that among the Y-family polymerases, hPol $\eta$ and hPol $\iota$ could contribute to error-prone bypass of OPdA while the catalytic subunit of hPol $\kappa$ (residues 19−526) is probably associated with accurate bypass. Highly impaired T7 (exo$^-$) DNA replicative polymerase activity suggests the ability of OPdA to hinder normal replication by some families of polymerases. Additionally, the block of hPol $\beta$ activity indicates this polymerase's active site has unique interactions with OPdA that result in inhibition of enzyme activity. Taken together, these studies indicate that OPdA is not highly mutagenic but may impair or block DNA polymerase activity *in vivo*.

## ■ AUTHOR INFORMATION

### Corresponding Author

*Department of Biochemistry, Vanderbilt University School of Medicine, Nashville, TN 37232-0146. E-mail: larry.marnett@vanderbilt.edu. Telephone: (615) 343-7329. Fax: (615) 343-7534.

### Author Contributions

L.M. and S.C.S. contributed equally to this work.

### Funding

This work was supported by research grants from the National Institutes of Health [F32 CA159701 (S.C.S.), R01 ES005355 (C.J.R.), R01 ES010375 and R01 ES010546 (F.P.G.), R00 GM084460 (R.L.E.), and R37 CA087819 (L.J.M.)].

### Notes

The authors declare no competing financial interest.

## ■ ACKNOWLEDGMENTS

We thank Carol Rouzer for editing the manuscript, Philip Kingsley for assistance with both mass spectrometric and HPLC analyses, and Orrette Wauchope for assistance with HPLC analysis. We are grateful to Sam Wilson of the National Institute for Environmental Health Sciences for a generous gift of purified hPol $\beta$.

## ■ ABBREVIATIONS

dNTPs, deoxyribonucleoside triphosphates; DTT, dithiothreitol; Kf, Klenow fragment of DNA polymerase I; Kf$^-$, Klenow fragment exonuclease deficient; MDA, malondialdehyde; $M_1dG$, 3-(2′-deoxy-$\beta$-D-*erythro*-pentofuranosyl)pyrimido[1,2-*a*]purin-10(3*H*)-one; OPdA, $N^6$-(oxopropenyl)-2′-deoxyadenosine; OPdC, $N^4$-(oxopropenyl)-2′-deoxycytidine; hPol $\eta$, human DNA polymerase $\eta$, amino acids 1−437; hPol $\iota$, human DNA polymerase $\iota$, amino acids 1−420; hPol $\kappa$, human DNA polymerase $\kappa$; hPol $\beta$, human DNA polymerase $\beta$; ACN, acetonitrile; TEAA, triethylammonium acetate.

## ■ REFERENCES

(1) Marnett, L. J. (2000) Oxyradicals and DNA damage. *Carcinogenesis 21*, 361−370.

(2) Marnett, L. J., Riggins, J. N., and West, J. D. (2003) Endogenous generation of reactive oxidants and electrophiles and their reactions with DNA and protein. *J. Clin. Invest. 111*, 583−593.

(3) Dedon, P. C., Plastaras, J. P., Rouzer, C. A., and Marnett, L. J. (1998) Indirect mutagenesis by oxidative DNA damage: Formation of the pyrimidopurinone adduct of deoxyguanosine by base propenal. *Proc. Natl. Acad. Sci. U.S.A. 95*, 11113−11116.

(4) Stone, K., Ksebati, M. B., and Marnett, L. J. (1990) Investigation of the adducts formed by reaction of malondialdehyde with adenosine. *Chem. Res. Toxicol. 3*, 33−38.

(5) Stone, K., Uzieblo, A., and Marnett, L. J. (1990) Studies of the reaction of malondialdehyde with cytosine nucleosides. *Chem. Res. Toxicol. 3*, 467−472.

(6) Chaudhary, A. K., Reddy, G. R., Blair, I. A., and Marnett, L. J. (1996) Characterization of an N6-oxopropenyl-2′-deoxyadenosine adduct in malondialdehyde-modified DNA using liquid chromatography/electrospray ionization tandem mass spectrometry. *Carcinogenesis 17*, 1167−1170.

(7) Mao, H., Schnetz-Boutaud, N. C., Weisenseel, J. P., Marnett, L. J., and Stone, M. P. (1999) Duplex DNA catalyzes the chemical rearrangement of a malondialdehyde deoxyguanosine adduct. *Proc. Natl. Acad. Sci. U.S.A. 96*, 6615−6620.

(8) Hashim, M. F., Riggins, J. N., Schnetz-Boutaud, N., Voehler, M., Stone, M. P., and Marnett, L. J. (2004) In vitro bypass of malondialdehyde-deoxyguanosine adducts: Differential base selection during extension by the Klenow fragment of DNA polymerase I is the critical determinant of replication outcome. *Biochemistry 43*, 11828−11835.

(9) Lehmann, A. R. (2002) Replication of damaged DNA in mammalian cells: New solutions to an old problem. *Mutat. Res. 509*, 23−34.

(10) Prakash, S., Johnson, R. E., and Prakash, L. (2005) Eukaryotic translesion synthesis DNA polymerases: Specificity of structure and function. *Annu. Rev. Biochem. 74*, 317−353.

(11) Benamira, M., Johnson, K., Chaudhary, A., Bruner, K., Tibbetts, C., and Marnett, L. J. (1995) Induction of mutations by replication of malondialdehyde-modified M13 DNA in *Escherichia coli*: Determination of the extent of DNA modification, genetic requirements for mutagenesis, and types of mutations induced. *Carcinogenesis 16*, 93−99.

(12) Ohmori, H., Friedberg, E. C., Fuchs, R. P., Goodman, M. F., Hanaoka, F., Hinkle, D., Kunkel, T. A., Lawrence, C. W., Livneh, Z., Nohmi, T., Prakash, L., Prakash, S., Todo, T., Walker, G. C., Wang, Z., and Woodgate, R. (2001) The Y-family of DNA polymerases. *Mol. Cell 8*, 7−8.

(13) Burgers, P. M., Koonin, E. V., Bruford, E., Blanco, L., Burtis, K. C., Christman, M. F., Copeland, W. C., Friedberg, E. C., Hanaoka, F., Hinkle, D. C., Lawrence, C. W., Nakanishi, M., Ohmori, H., Prakash, L., Prakash, S., Reynaud, C. A., Sugino, A., Todo, T., Wang, Z., Weill, J. C., and Woodgate, R. (2001) Eukaryotic DNA polymerases: Proposal for a revised nomenclature. *J. Biol. Chem. 276*, 43487−43490.

(14) Nelson, J. R., Lawrence, C. W., and Hinkle, D. C. (1996) Thymine-thymine dimer bypass by yeast DNA polymerase ζ. *Science 272*, 1646−1649.

(15) Hogg, M., Seki, M., Wood, R. D., Doublie, S., and Wallace, S. S. (2011) Lesion bypass activity of DNA polymerase θ (POLQ) is an intrinsic property of the pol domain and depends on unique sequence inserts. *J. Mol. Biol. 405*, 642−652.

(16) Wang, H., Kozekov, I. D., Kozekova, A., Tamura, P. J., Marnett, L. J., Harris, T. M., and Rizzo, C. J. (2006) Site-specific synthesis of oligonucleotides containing malondialdehyde adducts of deoxyguanosine and deoxyadenosine via a postsynthetic modification strategy. *Chem. Res. Toxicol. 19*, 1467−1474.

(17) Maddukuri, L., Ketkar, A., Eddy, S., Zafar, M. K., Griffin, W. C., and Eoff, R. L. (2012) Enhancement of human DNA polymerase η activity and fidelity is dependent upon a bipartite interaction with the Werner syndrome protein. *J. Biol. Chem. 287*, 42312−42323.

(18) Choi, J. Y., Angel, K. C., and Guengerich, F. P. (2006) Translesion synthesis across bulky N2-alkyl guanine DNA adducts by human DNA polymerase κ. *J. Biol. Chem. 281*, 21062−21072.

(19) Irimia, A., Eoff, R. L., Guengerich, F. P., and Egli, M. (2009) Structural and functional elucidation of the mechanism promoting error-prone synthesis by human DNA polymerase κ opposite the 7,8-dihydro-8-oxo-2′-deoxyguanosine adduct. *J. Biol. Chem. 284*, 22467−22480.

(20) Beard, W. A., and Wilson, S. H. (1995) Purification and domain-mapping of mammalian DNA polymerase β. *Methods Enzymol. 262*, 98−107.

(21) Pence, M. G., Choi, J. Y., Egli, M., and Guengerich, F. P. (2010) Structural basis for proficient incorporation of dTTP opposite O6-methylguanine by human DNA polymerase ι. *J. Biol. Chem. 285*, 40666−40672.

(22) Patel, S. S., Wong, I., and Johnson, K. A. (1991) Pre-steady-state kinetic analysis of processive DNA replication including complete characterization of an exonuclease-deficient mutant. *Biochemistry 30*, 511−525.

(23) Zang, H., Harris, T. M., and Guengerich, F. P. (2005) Kinetics of nucleotide incorporation opposite DNA bulky guanine N2 adducts by processive bacteriophage T7 DNA polymerase (exonuclease-) and HIV-1 reverse transcriptase. *J. Biol. Chem. 280*, 1165−1178.

(24) Furge, L. L., and Guengerich, F. P. (1997) Analysis of nucleotide insertion and extension at 8-oxo-7,8-dihydroguanine by replicative T7 polymerase exo- and human immunodeficiency virus-1 reverse transcriptase using steady-state and pre-steady-state kinetics. *Biochemistry 36*, 6475−6487.

(25) Choi, J. Y., Eoff, R. L., Pence, M. G., Wang, J., Martin, M. V., Kim, E. J., Folkmann, L. M., and Guengerich, F. P. (2011) Roles of the four DNA polymerases of the crenarchaeon *Sulfolobus solfataricus* and accessory proteins in DNA replication. *J. Biol. Chem. 286*, 31180−31193.

(26) Szekely, J., Rizzo, C. J., and Marnett, L. J. (2008) Chemical properties of oxopropenyl adducts of purine and pyrimidine nucleosides and their reactivity toward amino acid cross-link formation. *J. Am. Chem. Soc. 130*, 2195−2201.

(27) Waters, L. S., Minesinger, B. K., Wiltrout, M. E., D'Souza, S., Woodruff, R. V., and Walker, G. C. (2009) Eukaryotic translesion polymerases and their roles and regulation in DNA damage tolerance. *Microbiol. Mol. Biol. Rev. 73*, 134−154.

(28) Maddukuri, L., Eoff, R. L., Choi, J. Y., Rizzo, C. J., Guengerich, F. P., and Marnett, L. J. (2010) In vitro bypass of the major malondialdehyde- and base propenal-derived DNA adduct by human Y-family DNA polymerases κ, ι, and Rev1. *Biochemistry 49*, 8415−8424.

(29) Goodman, M. F. (2002) Error-prone repair DNA polymerases in prokaryotes and eukaryotes. *Annu. Rev. Biochem. 71*, 17−50.

(30) Tissier, A., McDonald, J. P., Frank, E. G., and Woodgate, R. (2000) poliota, a remarkably error-prone human DNA polymerase. *Genes Dev. 14*, 1642−1650.

(31) Woodside, A. M., and Guengerich, F. P. (2002) Misincorporation and stalling at O(6)-methylguanine and O(6)-benzylguanine: Evidence for inactive polymerase complexes. *Biochemistry 41*, 1039−1050.

(32) Choi, J. Y., and Guengerich, F. P. (2004) Analysis of the effect of bulk at N2-alkylguanine DNA adducts on catalytic efficiency and fidelity of the processive DNA polymerases bacteriophage T7 exonuclease- and HIV-1 reverse transcriptase. *J. Biol. Chem. 279*, 19217−19229.

(33) Hoffmann, J. S., Pillaire, M. J., Maga, G., Podust, V., Hubscher, U., and Villani, G. (1995) DNA polymerase β bypasses in vitro a single d(GpG)-cisplatin adduct placed on codon 13 of the HRAS gene. *Proc. Natl. Acad. Sci. U.S.A. 92*, 5356−5360.

(34) Hashim, M. F., Schnetz-Boutaud, N., and Marnett, L. J. (1997) Replication of template-primers containing propanodeoxyguanosine by DNA polymerase β. Induction of base pair substitution and frameshift mutations by template slippage and deoxynucleoside triphosphate stabilization. *J. Biol. Chem. 272*, 20205−20212.